

Nonparametric Quantile-Based Causal Discovery

Natasa Tagasovska ^{*} Thibault Vatter [†]
 Valérie Chavez-Demoulin[‡]

February 11, 2022

Abstract

Telling cause from effect using observational data is a challenging problem, especially in the bivariate case. Contemporary methods often assume an independence between the cause and the generating mechanism of the effect given the cause. From this postulate, they derive asymmetries to uncover causal relationships. In this work, we propose such an approach, based on the link between Kolmogorov complexity and quantile scoring. We use a nonparametric conditional quantile estimator based on copulas to implement our procedure, thus avoiding restrictive assumptions about the joint distribution between cause and effect. In an extensive study on real and synthetic data, we show that quantile copula causal discovery (QCCD) compares favorably to state-of-the-art methods, while at the same time being computationally efficient and scalable.

Keywords: causal discovery, quantile scoring, minimum description length, nonparametric, copula

1 Introduction

Motivated by the usefulness of causal inference in almost any field of science, an increasing body of research has contributed towards understanding the generative processes behind data. The aim is the elevation of learning models towards more powerful interpretations: from correlations and dependencies towards *causation* (Pearl, 2009, Pearl et al., 2016, Lopez-Paz, 2016).

^{*}Department of Information Systems, HEC Lausanne. E-mail: natasa.tagasovska@unil.ch

[†]Department of Statistics. Columbia University. E-mail: tv2233@columbia.edu

[‡]Department of Operations, HEC Lausanne. E-mail: valerie.chavez@unil.ch

While the golden standard for causal discovery is randomized control trials (Fisher, 1936), experiments or interventions in a system are often prohibitively expensive, unethical or, in many cases, impossible. In this context, an alternative is to use observational data to infer causal relationships (Maathuis and Nandy, 2016). This subtle and challenging task has been tackled by many, often relying on testing conditional independence and backed up by heuristics (Maathuis and Nandy, 2016, Spirtes and Zhang, 2016, Peters et al., 2017).

Borrowing from structural equations and graphical models, structural causal models (SCMs, Pearl et al., 2016, Peters et al., 2017) represent the causal structure of variables X_1, \dots, X_d using equations such as

$$X_c = f_c(X_{PA(p), \mathcal{G}}, E_c), \quad c \in \{1, \dots, d\}$$

where

- f_c is a causal mechanism linking the child (i.e., effect) X_c to its parents (i.e., direct causes) $X_{PA(p), \mathcal{G}}$,
- E_c is another variable independent of $X_{PA(p), \mathcal{G}}$,
- and \mathcal{G} is the directed graph obtained from drawing arrows from parents to their children.

Further complications arise when observing only two variables. In this case, one cannot distinguish between latent confounding ($X \leftarrow Z \rightarrow Y$) and direct causation ($X \rightarrow Y$ or $X \leftarrow Y$) without additional assumptions (Lopez-Paz et al., 2015). A possible solution to this open question is to impose certain model restrictions. For example, (non-)linear additive noise models, with $Y = f(X) + E_Y$, provide a foundation for establishing *identifiability* (Shimizu et al., 2006, Hoyer et al., 2009, Peters et al., 2011). An extension is the post non-linear model (Zhang and Hyvärinen, 2009), namely $Y = g(f(X) + E_Y)$ with g being an invertible function. Another line of work avoids functional restrictions by relying on the *independence of cause and mechanism* postulate (Schölkopf et al., 2012, Peters et al., 2017):

Postulate 1 (Sgouritsa et al. 2015). *The marginal distribution of the cause and the conditional distribution of the effect given the cause corresponding to independent mechanisms of nature, are independent (i.e., they contain no information about each other).*

IGCI (Janzing et al., 2012), one of the best performing algorithms in a recent benchmarking study (Mooij et al., 2016), uses the postulate directly for causal discovery. Alternatively, Mooij et al. (2010), Janzing and Schölkopf (2010) reformulate the postulate through asymmetries in Kolmogorov complexities (Kolmogorov, 1963) between marginal and conditionals distributions. However, the halting problem (Turing, 1937, 1938) implies that the Kolmogorov complexity is not computable, and approximations or proxies have to be derived to make the

concept practical. In this context, Mooij et al. (2010) proposes an approximation based on the minimum message length (MML) principle using Bayesian priors, and EMD (Chen et al., 2014) and FT (Liu and Chan, 2017) are based on embeddings from reproducing kernel hilbert space. A related line of work suggests using the minimum description length (MDL, Rissanen, 1978) principle as a proxy for Kolmogorov complexity: ORIGO (Budhathoki and Vreeken, 2017) uses MDL for causal discovery on binary data, and Slope (Marx and Vreeken, 2017) implements local and global functional relations using MDL-based regression and is suitable for continuous data.

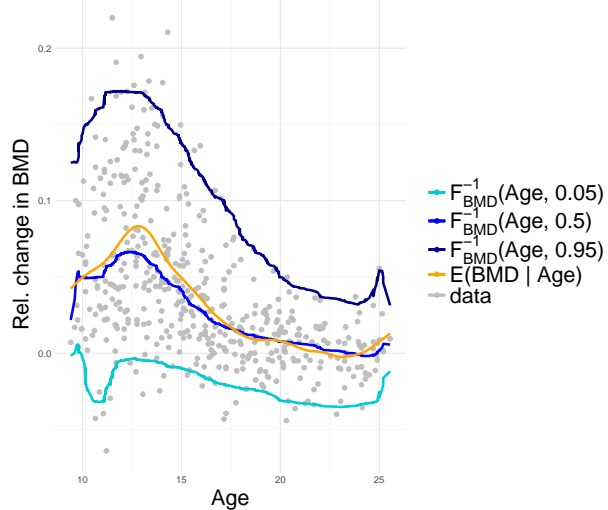


Figure 1: Conditional mean (orange) and quantiles (blues).

In this work, we build on a similar idea, using *quantile scoring* as a proxy for the Kolmogorov complexity through the MDL principle. Figure 1 motivates the use of quantiles in discovering causal relationship: the conditional mean provides the central tendency, but the entire distribution of change in bone mineral density (BMD) varies according to age. In this context, conditional quantiles provide a more detailed picture. For instance, it is visually obvious that the variance and positive skew of the BMD distribution are larger between 10 and 15 years than between 20 and 25. For such a dataset, distributional features other than the conditional mean can help causal discovery. To the best of our knowledge, quantiles have only been mentioned in a somewhat related context by Heinze-Deml et al. (2017), where predictions are used to exploit the invariance of causal models across different environments. As opposed to Heinze-Deml et al. (2017), our method uses an asymmetry directly derived from the postulate, and therefore does not require additional variables for the environment.

To avoid the restrictive assumptions imposed by standard quantile regression techniques, we estimate conditional quantiles fully nonparametrically using *copulas*. Since the introduction of the pitfalls of correlations (Embrechts et al., 1999), there has been a growing literature on copula-based methodology and applications in the statistics community. In a nutshell, copulas allow to flexibly model the dependence structure between random variables, while avoiding assumptions

about the scales, functional forms, or other restrictions imposed when dealing with marginal distributions. More recently, copulas made their way into the machine learning research as well (Liu et al., 2009, Elidan, 2013, Lopez-Paz et al., 2013, Tran et al., 2015, Lopez-Paz, 2016, Chang et al., 2016). In the context of causal inference for multivariate data, copulas have previously been explored in the Gaussian copula setting (Harris and Drton, 2013, Cui et al., 2016) or with pair-copula constructions as in Bauer and Czado (2016), Pircalabelu et al. (2017), Müller and Czado (2017). However, such approaches are not targeted at pairwise causal discovery.

To the best of our knowledge, we are the first to explore the idea of using conditional quantiles to distinguish cause from effect in bivariate observational data. Our main contributions are:

- a new method based on quantile scoring to determine the causal direction in bivariate datasets without restricting assumption on the class of possible causal mechanisms,
- a theoretical analysis justifying its usage,
- and *quantile copula causal discovery* (QCCD), an efficient algorithmic implementation allowing extensions to higher-dimensional datasets.

The rest of the paper is organized as follows. Section 2 introduces quantile scoring from a decision-theoretic perspective. Section 2.2 then building upon the link between quantile scoring and Kolmogorov complexity to formulate the quantile-based causal decision rule. Section 2.3, Section 2.4 and Section 2.5 further explains the proposed methodology and its implementation with nonparametric copulas. Section 3 presents a set of experiments on real and simulated datasets. In Section 4, we briefly explore extensions of our method to multi-variable case and we conclude in Section 5.

2 Nonparametric causal discovery using quantiles and copulas

In this section, we develop our quantile-based method for distinguishing between cause and effect from continuous and discrete observational data. We restrict ourselves to bivariate cases by considering pairs of univariate random variables. We further simplify the problem by assuming no confounding, no selection bias and no feedback.

2.1 Quantile Scoring

To introduce our score for quantile-based causal discovery, we first describe its statistical decision-theoretic roots and refer to Gneiting (2011) for more details. Let I be the range of potential outcomes (e.g., $I = \mathbb{R}$) and $Z \in I$ be a random variable

(r.v.) with distribution $F \in \mathcal{F}$, where \mathcal{F} is a family of distributions taking values in I . In this context, a *scoring function* is then any map $S : I \times I \rightarrow [0, \infty)$, and an *optimal point forecast* under S is then a minimizer of the expected score, namely

$$\hat{z} = \operatorname{argmin}_z \mathbb{E}_F [S(z, Z)].$$

Let a *functional* T is any mapping $F \rightarrow T(F) \subseteq I$.

Definition 1 (Consistent scoring function). *A scoring function S is said to be consistent for T relative to \mathcal{F} if*

$$\mathbb{E}_F [S(t, Z)] \leq \mathbb{E}_F [S(z, Z)],$$

for all $F \in \mathcal{F}$, $t \in T(F)$ and $z \in I$. Furthermore, S is strictly consistent if it is consistent and equality implies that $t \in T(F)$.

Example 1 (Mean and squared loss). Let the mean be the functional $\mu(F) = \mathbb{E}_F [Z]$ and the squared-loss be the scoring function $S(z_1, z_2) = (z_1 - z_2)^2$. Then μ is the optimal point forecast under S , and S is consistent for μ .

This example helps building an intuition about the links between functionals, optimal point forecasts and consistent scoring functions. These relationships can be further formalized as follow:

Theorem 1 (Gneiting 2011). *For any $F \in \mathcal{F}$ and $T(F)$, $t \in T(F)$ is an optimal point forecast under S if and only if S is consistent for $T(F)$ relative to \mathcal{F} .*

In other words, there is a duality between point forecast optimality and consistency, or between making and evaluating point forecasts.

Example 2 (Quantile and quantile scoring). The τ -quantile μ_τ is the functional

$$\mu_\tau(F) = F^{-1}(\tau) = \operatorname{arginf}_\mu \{\mu \mid F(\mu) = \tau\}.$$

If i is an increasing function (e.g., the identity $i(z) = z$) and \mathbb{I} is the indicator function, then the scoring function

$$S(z_1, z_2) = (\mathbb{I}\{z_1 \geq z_2\} - \tau)(i(z_1) - i(z_2)), \quad (1)$$

is consistent for the τ -quantile (Gneiting, 2011).

Denoting by $F_{Y|X}$ and $F_{X|Y}$ the conditional distributions of Y given X and X

given Y , we let

$$\begin{cases} S_{Y|X}(\tau) &= \mathbb{E} \left[S(F_{Y|X}^{-1}(X, \tau), Y) \right], \\ S_{X|Y}(\tau) &= \mathbb{E} \left[S(F_{X|Y}^{-1}(\tau, Y), X) \right] \end{cases} \quad (2)$$

for $\tau \in [0, 1]$ and where S is as in (1) using the identity $i(z) = z$, and inverse functions are with respect to τ . In the next section, we link asymmetries between in the *quantile scores* $S_{Y|X}(\tau)$ and $S_{X|Y}(\tau)$ to asymmetries in Kolmogorov complexity using the MDL principle.

2.2 From Quantile Scoring to Kolmogorov complexity

For a distribution F , the Kolmogorov complexity $K(F)$ is the length of the shortest computer program producing F as output. This concept can be leveraged for causal discovery through the following theorem:

Theorem 2 (Mooij et al. 2010). *Let X and Y be two random variables. If X is a cause of Y , then $K(F_X) + K(F_{Y|X}) \leq K(F_Y) + K(F_{X|Y})$ holds, up to an additive constant.*

Stated differently, the most likely causal direction between X and Y can be recognized by the lowest value of the Kolmogorov complexity. Since the Kolmogorov complexity is not computable, we use the MDL principle, known as the practical version of Kolmogorov complexity, as a proxy. According to the MDL principle, the “best” model is the one providing an optimal compression of the data, allowing to store information using the shortest code length (CL). The following theorem related asymmetries in quantile scores to asymmetries in code length.

Theorem 3. *Let $(X, Y) \sim F$ be a bivariate random vector and \hat{F} be an estimate of F based on a dataset $\{(X_i, Y_i)\}_{i=1}^n$. If \hat{F}_X , \hat{F}_Y , $\hat{F}_{X|Y}$ and $\hat{F}_{Y|X}$ are all derived from \hat{F} , then*

$$CL_{Y|X}(\tau) \leq CL_{X|Y}(\tau) \iff \hat{S}_{Y|X}(\tau) \leq \hat{S}_{X|Y}(\tau)$$

for all $\tau \in [0, 1]$, where

$$\begin{cases} \hat{S}_{Y|X}(\tau) &= \frac{1}{n} \sum_{i=1}^n S(\hat{F}_{Y|X}^{-1}(X_i, \tau), Y_i), \\ \hat{S}_{X|Y}(\tau) &= \frac{1}{n} \sum_{i=1}^n S(\hat{F}_{X|Y}^{-1}(\tau, Y_i), X_i) \end{cases}.$$

Proof The code length CL can be decomposed into two parts: the code length of the model under consideration and the leftover information, not explained by the model (see e.g., Hansen and Yu, 2001). As such, for a given quantile level τ ,

we can write:

$$\begin{cases} CL_{Y|X}(\tau) = CL(\widehat{F}_{Y|X}) + CL(E_Y, \tau), \\ CL_{X|Y}(\tau) = CL(\widehat{F}_{X|Y}) + CL(E_X, \tau) \end{cases}, \quad (3)$$

where $E_{Y,i} = Y_i - \widehat{F}_{Y|X}^{-1}(X_i, \tau)$ and $E_{X,i} = X_i - \widehat{F}_{X|Y}^{-1}(Y_i, \tau)$ for $i \in \{1, \dots, n\}$. Because all estimators are derived from the same \widehat{F} , we have that the code lengths corresponding to the models in both directions are equal, that is

$$CL(\widehat{F}_{Y|X}) = CL(\widehat{F}_{X|Y}) = CL(\widehat{F}). \quad (4)$$

Furthermore, following Aue et al. (2014), the code lengths to encode the portions of the data unexplained by the models can be written as

$$\begin{cases} CL(E_Y, \tau) = n\widehat{S}_{Y|X}(\tau), \\ CL(E_X, \tau) = n\widehat{S}_{X|Y}(\tau) \end{cases}. \quad (5)$$

Combining (3), (4) and (5) proves the theorem. \square

Stated differently, Theorem 3 implies that minimizing the code length is equivalent to minimizing the quantile score. Hence, because of the MDL principle, the causal direction can be inferred from the lowest quantile score. We thus define our quantile-based score for a given τ as

$$S_{X \rightarrow Y}(\tau) = \frac{\widehat{S}_{X|Y}(\tau)}{\widehat{S}_{Y|X}(\tau) + \widehat{S}_{X|Y}(\tau)} \quad (6)$$

with $S_{X \rightarrow Y}(\tau) \in [0, 1]$ and $S_{Y \rightarrow X}(\tau) = 1 - S_{X \rightarrow Y}(\tau)$. Then, we use the following rule for causal discovery:

Corollary 1 (Quantile-based causal discovery). *If $S_{X \rightarrow Y}(\tau) > 0.5$, conclude that X causes Y . If $S_{Y \rightarrow X}(\tau) > 0.5$, conclude that Y causes X . Otherwise, do not decide.*

Note that this score and rule are similar to the ideas in Budhathoki and Vreeken (2017), which propose a normalization based on the sum of the description lengths for the marginal distributions, and write

$$\Delta_{X \rightarrow Y} = \frac{CL_X + CL_{Y|X}}{CL_X + CL_Y}.$$

They then infer X causes Y if $\Delta_{X \rightarrow Y} \leq \Delta_{Y \rightarrow X}$, that Y causes X if $\Delta_{X \rightarrow Y} \geq \Delta_{Y \rightarrow X}$, and do not decide if otherwise. Under the conditions of Theorem 3, it is clear that $\Delta_{X \rightarrow Y} \geq \Delta_{Y \rightarrow X}$ if and only if $S_{Y \rightarrow X}(\tau) \geq S_{X \rightarrow Y}(\tau)$.

Due to the invariance of the true causal model given different values of the conditioning variable, we expect outputs of our causal rule to agree over different quantile levels. For instance, in the dataset of Figure 1, while the conditional

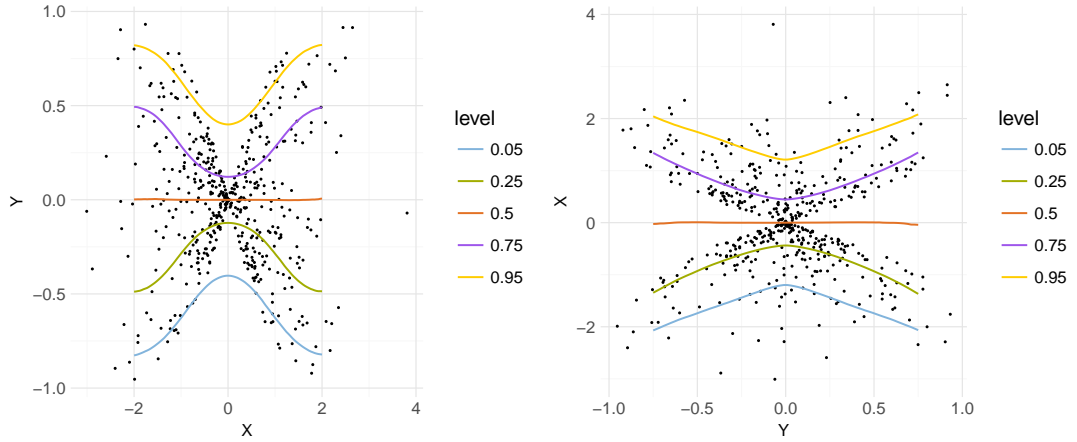


Figure 2: A sample of 500 observations of $Y = f(X) E_Y$, where $X \sim N(0, 1)$, $f(x) = \tanh(x)$ and $E_Y \sim U(0, 1)$, with conditional quantiles $F_{Y|X}^{-1}(x, \tau)$ (left) and $F_{X|Y}^{-1}(\tau, y)$ (right) for different values of the level τ .

Table 1: Quantile-based scores obtained with 300 repetitions of the setup of Figure 2 (standard deviations in parenthesis). All values are multiplied by 100, except in the first column.

τ	$\widehat{S}_{X Y}(\tau)$	$\widehat{S}_{Y X}(\tau)$	$S_{X \rightarrow Y}(\tau)$
0.05	9.4 (0.5)	3 (0.1)	75.7 (1)
0.25	28.7 (1.2)	10.6 (0.4)	73 (0.8)
0.5	38.4 (1.5)	13.6 (0.5)	73.8 (0.7)
0.75	28.8 (1.2)	10.6 (0.4)	73.1 (0.8)
0.95	9.5 (0.5)	3 (0.1)	75.8 (1)

distribution may vary for different age groups, the causal relation (i.e., age causes change in bone mineral density) does not. To aggregate the results of different causal decisions, we extend the score of (6) to

$$S_{X \rightarrow Y} = \int_{[0,1]} S_{X \rightarrow Y}(\tau) d\tau. \quad (7)$$

By pooling results at different quantile levels, we better describe the marginal and conditional distributions, hence increasing confidence in the causal decision.

Figure 2 and Table 1 give an intuition about (6) and (7). In Figure 2, a toy example of a causal simulation setup is described and shown for a sample of 500 observations. Furthermore, distributions of the effect conditionally on the cause, and of the cause conditionally on the effect, are described through five quantile levels. In Table 1, we see that $\widehat{S}_{X|Y}(\tau) > \widehat{S}_{Y|X}(\tau)$ and that $S_{X \rightarrow Y}(\tau) > 0.5$ at all quantile levels, hence implying the correct causal decision.

2.3 Predicting quantiles with copulas

To leverage Theorem 3 and Corollary 1 for causal discovery, a model of F , the joint distribution of X and Y is required. Furthermore, it has to yield computable expressions for all conditional quantiles. While not the only statistical model satisfying this condition, copulas, namely multivariate distributions with uniform margins, represent an appealing alternative.

By the theorem of Sklar (1959), any F can be represented by its marginal distributions F_X, F_Y and a copula C , which is the joint distribution of $(U, V) = (F_X(X), F_Y(Y))$. In other words, for any F , there exists a C such that

$$F(x, y) = C(F_X(x), F_Y(y)) \quad (8)$$

for each $(x, y) \in \mathbb{R}^2$. Moreover, if all the distributions are continuous, then C is unique.

Following Joe (1996), (8) leads to a useful representation of the distributions of $Y|X$ and $X|Y$, namely

$$\begin{aligned} F_{Y|X}(x, y) &= P(Y \leq y | X = x) \\ &= P(V \leq v | U = u) \\ &= \partial_u C(u, v), \end{aligned}$$

where $\partial_u C(u, v) = \frac{\partial C(u, v)}{\partial u}$, $u = F_X(x)$, and $v = F_Y(y)$, and similarly $F_{X|Y}(x, y) = \frac{\partial C(u, v)}{\partial v} = \partial_v C(u, v)$. This means that conditional distributions can be evaluated by taking partial derivatives of the copula function. The τ -quantiles of Y given $X = x$ and of X given $Y = y$ can then be written as

$$\begin{cases} F_{Y|X}^{-1}(x, \tau) = F_Y^{-1}((\partial_u C)^{-1}(u, \tau)), \\ F_{X|Y}^{-1}(\tau, y) = F_X^{-1}((\partial_v C)^{-1}(\tau, v)) \end{cases} \quad (9)$$

where inverse functions of the copula derivatives are with respect to τ . Using (9), one can then compute all τ -quantiles using the marginal distributions and the copula.

2.4 Estimation

Assume that we have n i.i.d. random variables $\{(X_1, Y_1), \dots, (X_n, Y_n)\}$. To avoid relying on restrictive assumptions, $S_{X \rightarrow Y}$ and $S_{Y \rightarrow X}$ are estimated completely nonparametrically.

First, note that, if all the considered distributions are differentiable, (8) implies

$$f(x, y) = c\{F_X(x), F_Y(y)\}f_X(x)f_Y(y), \quad (10)$$

where f, c, f_X, f_Y are the densities corresponding to F, C, F_X, F_Y respectively. Equation (10) has an important implication for inference: because the right-hand side is a product, the joint log-likelihood can be written as a sum between the

log-likelihood of each margin and the log-likelihood of the copula. This fact can be conveniently exploited in a two-step procedure:

- (i) Estimate the margins separately to obtain \hat{F}_X and \hat{F}_Y .
- (ii) Take the probability integral transform of the data using those margins, namely define $\hat{U}_i = \hat{F}_X(X_i)$ and $\hat{V}_i = \hat{F}_Y(Y_i)$, to estimate \hat{C} .

For the first step, we simply use the empirical distributions

$$\begin{cases} \hat{F}_X(x) = \frac{1}{n+1} \sum_{i=1}^n \mathbb{I}\{X_i \leq x\}, \\ \hat{F}_Y(y) = \frac{1}{n+1} \sum_{i=1}^n \mathbb{I}\{Y_i \leq y\} \end{cases}$$

where $n+1$ is used instead of n in the copula context to avoid boundary problems. Discrete datasets are handled by *jittering*, namely breaking ties at random. As for the second step, since usual nonparametric estimators are targeted at densities with unbounded support, they are unsuited to copula densities restricted to $[0, 1]^2$. To get around this issue, Scaillet et al. (2007) suggests to first transform the data to standard normal margins, and then use any nonparametric estimator suited to unbounded densities. The transformation estimator of the copula density $c(u, v)$ is then defined as

$$\hat{c}(u, v) = \frac{\hat{g}(\Phi^{-1}(u) - \Phi^{-1}(\hat{U}_i), \Phi^{-1}(v) - \Phi^{-1}(\hat{V}_i))}{\phi(\Phi^{-1}(u))\phi(\Phi^{-1}(v))}, \quad (11)$$

where $\hat{U}_i = \hat{F}_X(X_i)$, $\hat{V}_i = \hat{F}_Y(Y_i)$, \hat{g} is a bivariate nonparametric estimator and ϕ, Φ denote respectively the standard normal density and distribution.

Denoting $Z_i = (\Phi^{-1}(\hat{U}_i), \Phi^{-1}(\hat{V}_i))$ and $z = (\Phi^{-1}(u), \Phi^{-1}(v))$. the goal is to obtain the density for any $z = (z_1, z_2) \in \mathbb{R}^2$ from the sample $\{Z_i\}_{i=1}^n$ with $Z_i = (Z_{i,1}, Z_{i,2})$. With the bivariate Gaussian kernel

$$W_{B_n}(z_2, z_2) = \frac{\exp(-z^\top B_n^{-1} z / 2)}{2\pi \det(B_n)^{1/2}}$$

for a positive definite bandwidth matrix B_n , Scaillet et al. (2007) suggests to plug-in the usual bivariate kernel estimator of $g(z_1, z_2)$, namely

$$\hat{g}(z_1, z_2) = \frac{1}{n} \sum_{i=1}^n W_{B_n}(z_1 - Z_{i,1}, z_2 - Z_{i,2}), \quad (12)$$

into (11). The consistency and asymptotic normality of this approach are derived in Geenens et al. (2017).

2.5 Implementation

The transformation kernel estimator for bivariate copula densities is implemented in C++ as part of **vinecopulib** (Nagler and Vatter, 2017), an header-only

C++ library for copula models based on **Eigen** (Guennebaud et al., 2010) and **Boost** (Schäling, 2011). From (11), **vinecopulib** constructs and stores a 30×30 grid over $[0, 1]^2$ along with the evaluated density at the grid points. Then, a cubic-spline approximation allows to efficiently compute the copula distribution and its derivatives, namely $\widehat{C}(u, v)$, $\partial_u \widehat{C}(u, v)$ and $\partial_v \widehat{C}(u, v)$, as the integrals of the spline-approximation of the density admits an analytic expression. Finally, **vinecopulib** implements the numerical inversion of $\partial_u \widehat{C}(u, v)$ and $\partial_v \widehat{C}(u, v)$ to compute $(\partial_u \widehat{C})^{-1}(u, v)$ and $(\partial_v \widehat{C})^{-1}(u, v)$ by a vectorized version of the bisection method.

The second step of the implementation consists in estimating $S_{Y|X}(\tau)$, $S_{X|Y}(\tau)$, and $S_{X \rightarrow Y}$, namely plugging-in estimates of the marginal and derivatives of the copula in (9) and (1) to obtain

$$\begin{cases} \widehat{S}_{Y|X}(\tau) &= \frac{1}{n} \sum_{i=1}^n S(Y_i, \widehat{F}_Y^{-1}((\partial_u \widehat{C})^{-1}(\widehat{U}_i, \tau))), \\ \widehat{S}_{X|Y}(\tau) &= \frac{1}{n} \sum_{i=1}^n S(X_i, \widehat{F}_X^{-1}((\partial_v \widehat{C})^{-1}(\tau, \widehat{V}_i))). \end{cases}$$

As for estimating the final score, we use Legendre quadrature to approximate the integral over $[0, 1]$. In other words, denoting by $\{w_j, \tau_j\}_{j=1}^m$ the m pairs of quadrature weights and nodes, we use $\int_0^1 g(\tau) d\tau \approx \sum_{j=1}^m w_j g(\tau_j)$, which when plugged in (7) yields

$$\widehat{S}_{X \rightarrow Y} = \sum_{j=1}^m w_j \frac{\widehat{S}_{X|Y}(\tau_j)}{\widehat{S}_{Y|X}(\tau_j) + \widehat{S}_{X|Y}(\tau_j)}.$$

We implemented the *quantile copula causal discovery* (QCCD, see Algorithm 1) using the R (R Core Team, 2017) interface to **vinecopulib** called **rvinecopulib** (Nagler and Vatter, 2018), along with implies of \widehat{S} and Gauss-Legendre quadrature provided respectively in the packages **Hmisc** (Harrell Jr et al., 2017) and **statmod** (Smyth, 2005).

Computational complexity QCCD scales linearly with the size of input data as well as the number of quantiles used in the quadrature, i.e., the overall complexity is $\mathcal{O}(nm)$. As such, QCCD compares favorably to nonparametric methods relying on computationally intensive procedures, for instance based on kernels (Chen et al., 2014, Hernández-Lobato et al., 2016) or Gaussian processes (Hoyer et al., 2009, Mooij et al., 2010, Sgouritsa et al., 2015). The parameter m can be used to control for the trade-off between computation complexity and precision of the estimation. We recommend the value $m = 3$ which allows to capture variability in both location and scale. Setting $m = 1$ is essentially equivalent as using only the conditional median for causal discovery, a setting that is especially suitable for distributions with constant variance. In what follows, we report results for QCCD with $m = 3$.

Algorithm 1 Quantile Copula Causal Discovery

Input: i.i.d. observations $\{X_i, Y_i\}_{i=1}^n$ of the r.v. X and Y .

1. Get pseudo-observations by computing:

$$\begin{cases} \widehat{U}_i &= \frac{1}{n+1} \sum_{j=1}^n \mathbb{I}\{X_j \leq X_i\}, \\ \widehat{V}_i &= \frac{1}{n+1} \sum_{j=1}^n \mathbb{I}\{Y_j \leq Y_i\} \end{cases}$$

2. Estimate the copula nonparametrically to get:

$$\begin{cases} (\partial_u \widehat{C})^{-1}(u, v), \\ (\partial_v \widehat{C})^{-1}(u, v) \end{cases}$$

3. Compute the quadrature weights and nodes $\{w_j, \tau_j\}_{j=1}^m$.

4. Initialize score $s = 0$.

for $j = 1$ **to** m **do**

 Compute:

$$\begin{cases} \hat{S}_1 = \frac{1}{n} \sum_{i=1}^n S(\widehat{F}_Y^{-1}((\partial_u \widehat{C})^{-1}(\widehat{U}_i, \tau_j)), Y_i), \\ \hat{S}_2 = \frac{1}{n} \sum_{i=1}^n S(\widehat{F}_X^{-1}((\partial_v \widehat{C})^{-1}(\tau_j, \widehat{V}_i)), X_i) \end{cases}$$

$$s \rightarrow s + w_j \frac{\hat{S}_2}{\hat{S}_1 + \hat{S}_2}$$

end for

if $s > 0.5$ **then**

 Define causal discovery $d = X \rightarrow Y$.

else if $s < 0.5$ **then**

 Define causal discovery $d = Y \rightarrow X$.

else

 Define causal discovery $d = \text{undecided}$.

end if

Output: (d, s)

3 Experiments

Benchmarks For the simulated data, we first rely on the 4 scenarios Mooij et al. (2016): *SIM* (without confounder), *SIM-ln* (with low noise), *SIM-G* (with distributions close to Gaussian), and *SIM-c* (with latent confounder). There are 100 pairs of size $n = 1000$ in each, and we exclude *SIM-c* since it violates our assumptions from Section 2.

The second experiment compares different setups for non-linear additive noise (*AN*) models, namely

$$Y = f(X) + E_Y$$

for some deterministic function f with $E_Y \sim \mathcal{N}(0, \sigma)$, $X \sim \mathcal{N}(0, \sqrt{2})$, and $\sigma \sim \mathcal{U}[1/5, \sqrt{2/5}]$. In *AN*, f is an arbitrary non-linear function simulated using Gaussian processes (GP) as in Rasmussen and Williams (2006). Since the functions in *AN* are often non-injective, we include *AN-s* to exploring the behavior of QCCD in injective cases. In this setup, f are sigmoids as in Bühlmann et al. (2014).

The third experiment considers heteroskedastic (*HN*) data generating processes with both the mean and variance of the effect being functions of the cause, that is

$$Y = af(X) + g(X)E_Y,$$

where $a \sim \mathcal{U}[0.1, 0.9]$, and $g(X) = 1 + bX$ with $b \sim \mathcal{U}[0.1, 0.9]$, and E_Y as well as X similar as for additive noise models. *HN* and *HN-s* then correspond to the Gaussian processes and sigmoids described for *AN* and *AN-s*.

Finally, for the fourth experiment, we consider multiplicative models (*MN*) with

$$Y = f(X)E_Y$$

with $E_Y \sim \mathcal{U}(-1, 1)$ for *MN-U* and $E_Y \sim \mathcal{N}(0, 1)$ for *MN-G*.

In each of the second, third and fourth experiments, we simulate 100 pairs of size $n = 1000$. All pairs have equal weights with variable ordering according to a coin flip, therefore resulting in balanced datasets. Example datasets for each of the simulated experiments are shown as supplementary material (see Section 6.1).

For real data, we use the popular Tuebingen CE benchmark (Mooij et al., 2016), consisting of 106 pairs from 37 different domains, from which we consider only the 100 pairs that have univariate cause and effect variables.

Baselines On simulated data, we compare QCCD to state-of the-art approaches:

- RESIT (Peters et al., 2014), biCAM (Bühlmann et al., 2014), LinGaM (Shimizu et al., 2006) and GR-AN (Hernández-Lobato et al., 2016) are ANM-based,
- IGCI (Janzing and Schölkopf, 2010), EMD (Chen et al., 2014) and Slope (Marx and Vreeken, 2017) are based on the independence postulate.

We also consider other methods such as PNL-MLP Zhang and Hyvärinen (2009), GPI (Mooij et al., 2010), ANM Hoyer et al. (2009) and CURE Sgouritsa et al. (2015). For the real data benchmark, they are evaluated over 15 subsamples limited to 500 observations and results are then averaged. For the simulated experiments however, they are excluded due to slow execution.

Implementations and hyper parameters For IGCI, we use the original implementation of Janzing et al. (2012) with slope-based estimation and uniform reference measure. For LINGAM, we use the implementation of Peters et al. (2014), which also provides RESIT with GP regression paired and the HSIC independence test with a threshold value $\alpha = 0.05$. For CAM, we use Peters and Ernest (2015) with the default parameters. For GR-AN and EMD, we use the code of Hernández-Lobato et al. (2016). The parameters for EMD on simulated data are as in the original paper, $\lambda = 1e^{-3}$ and $\sigma = \frac{1}{5}S_m$ (S_m being the median of

distances across all input patterns). For the real data, the parameters are tuned and selected from the overall best results. For Slope, we use the implementation of Marx and Vreeken (2017) with local regression included in the fitting process. For PNL, GPI-MML, and ANM, we use the MATLAB implementation from the *Cause Effect Pairs Challenge FirfiD* (<https://github.com/ssamot/causality>), with the same setup as RESIT for ANM. Our code and datasets are available at <https://github.com/tagas/qccd>. Because there is no publicly available implementation of CURE, we show the results obtained by Marx and Vreeken (2017). All experiments are done with R version 3.4.1 on a MacBook Pro (mid 2015) with 16GB memory, 2.2 GHz Intel Core i7 and 250GB disk.

Evaluation metrics To evaluate and compare competing methods, as suggested in (Mooij et al., 2016), we use *accuracy* for forced-decision and the *area under the receiver operating curve* (ROC). We also use empharea under the precision-recall curve (PR) for *ranked-decision*. Due to lack of space, we present the results from all measures and methods on the real data only. For the simulated experiments, we show the accuracy, and refer to the supplementary material for ROC and PR results (see Section 6.2).

Results and discussion In Table 2, Table 3, Figure 3 and Figure 4 we compare the causal discovery algorithms across simulated datasets. From Table 2, we notice that QCCD has a consistent behavior: its accuracy is $> 75\%$ across all benchmarks, except SIM for which none of the algorithms but RESIT does better than a random classifier. From Table 3 and Figure 4, we observe that QCCD performs similarly well in terms of area under the ROC and PR curves. This can be explain by the fact that we use the confidence score (7) as a threshold for ranked decision. Since the scores are often high in these simulated experiments, they are translated into high values for the area under the ROC and PR curves. However, such high values are not unusual and sometimes observed for competing methods as well (see Section 6.2 in the supplementary material).

Table 2: Accuracy on simulated data.

	SIM	SIM-In	SIM-G	AN	AN-s	HN	HN-s	MN-U	MN-G
QCCD	0.49	0.77	0.76	1	1	1	1	1	0.82
IGCI	0.42	0.52	0.54	0.41	0.35	0.81	0.85	0.02	0.97
biCAM	0.57	0.87	0.81	1	1	0.78	0.47	0.04	0.03
Slope	0.45	0.47	0.48	0.18	0.28	0.62	0.74	0.07	0.96
RESIT	0.78	0.87	0.77	1	1	0.31	0.08	0.09	0.04
LINGAM	0.44	0.32	0.33	0.04	0.04	0	0.01	0	0.02
EMD	0.47	0.52	0.6	0.36	0.47	0.73	0.81	0.62	0.95
GR-AN	0.47	0.41	0.37	0.05	0.06	0.39	0.49	0.94	0.45

Table 3: Area under the ROC and PR curves for QCCD.

	SIM	SIM-In	SIM-G	AN	AN-s	HN	HN-s	MN-U	MN-G
ROC-AUC	0.56	0.89	0.89	1	1	1	1	1	0.91
PR-AUC	0.60	0.89	0.89	1	1	1	1	1	0.93

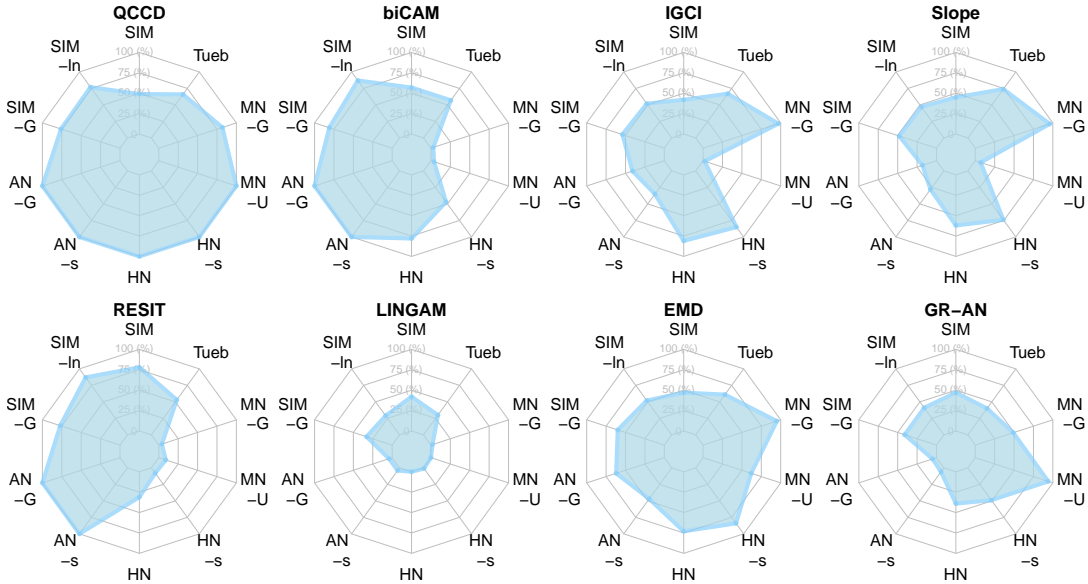


Figure 3: Radar plots of accuracy for QCCD and competitors.

As expected, most methods perform better when the generative model is closer to the assumptions they rely on. For instance, CAM and RESIT are highly accurate for AN pairs, while performing poorly for MN pairs. Similarly, LINGAM does not perform well on any of the datasets, which are all highly non-linear, hence violating its assumptions.

While ICGI performs well in HN scenarios, a possible reason for its poor performance in the AN scenarios may be an unsuited reference measure (i.e., uniform instead of Gaussian). However, selecting the reference measure is the most sensitive part of the method and is often as hard as selecting the right kernel/bandwidth for a specific task (Janzing et al., 2012, Mooij et al., 2016). EMD does well on the MN-G benchmark, but its accuracy drops when it comes to AN data. As for GR-AN, it does not perform well in either the SIM benchmarks or in the AN setting, the likely reason being the non-injectivity. However, it behaves better with multiplicative uniform noise. From this simulation study, we see that only QCCD handles well additive, multiplicative and heteroskedastic data.

With real data pairs, we notice from Table 4 that QCCD is highly competitive in terms of AUC and accuracy, with only Slope achieving better overall results. Probably the relevant score for this the real dataset is AUC-PR due to the imbalance of the class labels, there are 74 pairs with ground truth $X \rightarrow Y$ and only 26 $Y \rightarrow X$ causal directions. Moreover, the efficiency of our method is

Table 4: Evaluation metrics on the Tuebingen benchmark.

	QCCD	IGCI	biCAM	Slope	LINGAM	RESIT
Accuracy	0.66	0.67	0.57	0.74	0.3	0.53
ROC-AUC	0.69	0.68	0.58	0.83	0.41	0.59
PR-AUC	0.81	0.85	0.76	0.94	0.69	0.81
CPU(sec)	13 min.	2 sec.	10 sec.	25 min.	3.5 sec.	12 h
	EMD	GR-AN	GPI-MML	PNL-MLP	ANM	CURE
Accuracy	0.60 ± 2.8	0.40 ± 2.18	0.63 ± 2.38	0.64 ± 3.58	0.6 ± 1.76	0.6
ROC-AUC	0.62 ± 0	0.47 ± 0.02	0.69 ± 0.02	0.6 ± 0.04	0.50 ± 0.15	0.58
PR-AUC	0.83 ± 0	0.74 ± 0.02	0.87 ± 0.02	0.79 ± 0.01	0.71 ± 0	0.79
CPU(sec)	NA	NA	NA	NA	NA	NA

highlighted in the last row, where QCCD is able to go over the whole dataset in 13 minutes. As for other nonparametric methods, only IGCI is faster, Slope is twice as slow, RESIT 55 times, and the others could not go through the whole dataset and had to be averaged on subsamples due to slow execution.

4 Extensions of the pairwise method

Recent work by Goudet et al. (2017) suggests that pairwise and CPDAG (the skeleton and the *v*-structures of a graphical model) learning procedures can suitably complement each other. In this section, we follow similar approach to suggest an extension of QCCD to multivariate datasets: start from the CPAG resulting from another method, and then use QCCD to orient the edges. More specifically, we can perform the second step by obtaining a causal direction and confidence according to (7) in the decision for each edge. Then, we rank edges and include them in the graph sequentially, starting from the highest confidence, while checking the acyclicity of the resulting graph after each addition. Note that this approach also requires a final verification to test edge orientation and *v*-structures consistency (Goudet et al., 2017).

We explore this idea by using CAM to learn a CPDAG and then QCCD to orient its edges. The rationale is that, while Bühlmann et al. (2014) proves the consistency of CAM to learn the structure when assumptions are not met, QCCD is better in pairwise discoveries (see Section 3).

In a dataset on octet binary semi-conductors (Mandros et al., 2017), the target variable is the *energy difference* between rocksalt and zincblende crystal structures, with all other variables being causes according to Marx and Vreeken (2017). In the left and right panels of Figure 5, we present respectively the results of the CPDAG as recovered by CAM and of the above mentioned procedure. While CAM recovers 7 out of the 10 required edges, it reports 3 wrong directions, and QCCD orients all 7 edges correctly. If only pairs of variables are considered as in Marx and Vreeken (2017), QCCD gives the 10 correct decisions. As such, it is both reassuring that QCCD is able to correctly decide for the causal direction,

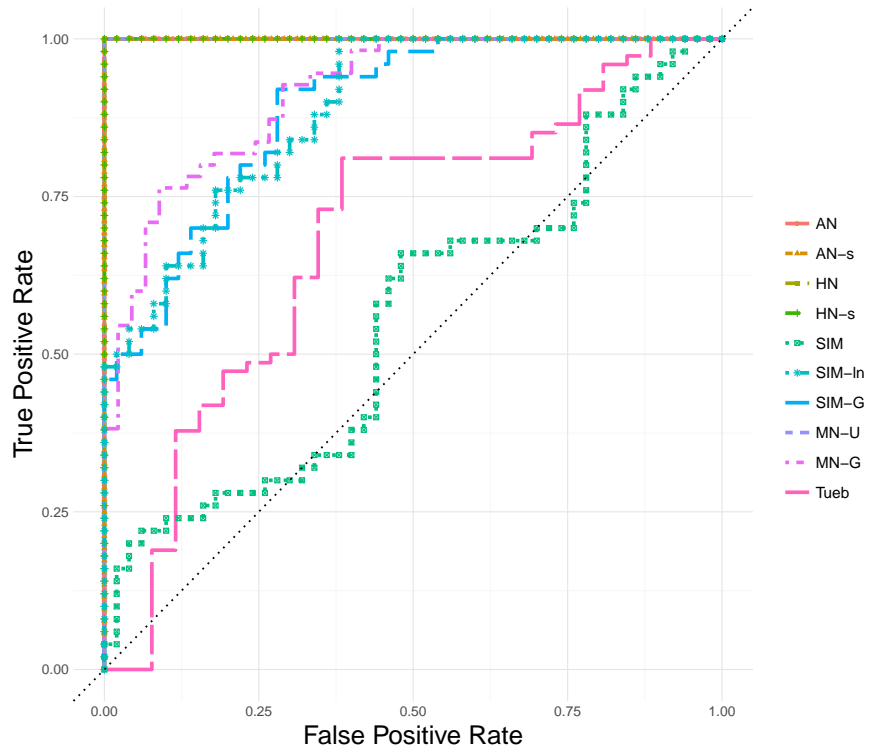


Figure 4: ROC curves for QCCD on different benchmarks.

even though other dependencies affect the pairwise causal relationships. While such results are promising, a consistent hybrid method extending QCCD to higher dimensional datasets is left for further work.

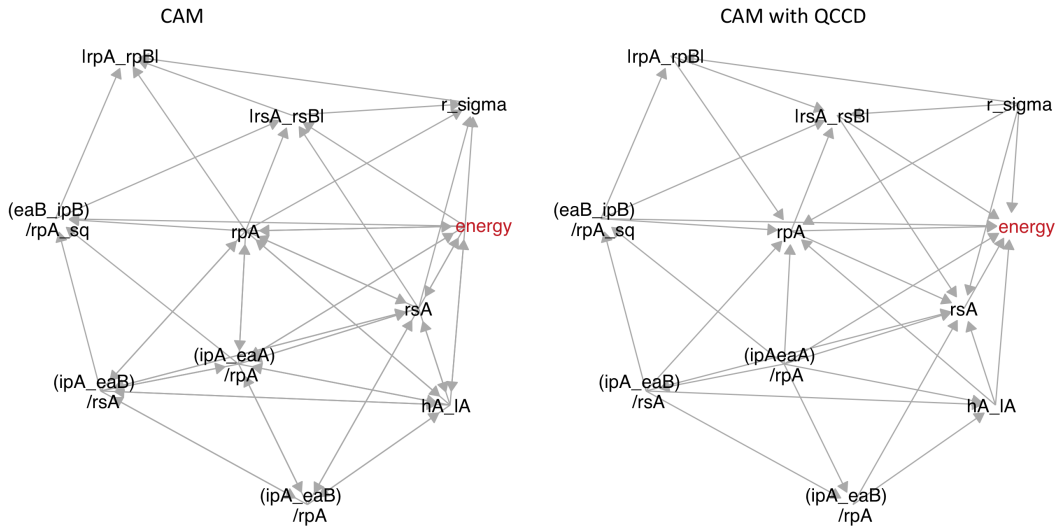


Figure 5: CPDAG and DAG for the Octet dataset.

5 Conclusion

In this work, we develop a causal discovery method based on conditional quantiles. We give a rigorous basis to the approach by showing its link to Kolmogorov complexity and therefore to the independence postulate. We propose QCCD, an effective implementation of our method based on nonparametric copulas. Studying QCCD extensively both with simulated and real datasets, we show that it compares favorably to state-of-the-art while methods. There are currently two directions that we are exploring to extend this work.

First, our theory allows for a modular approach to pairwise causal discovery: using different combinations of quantile regression approaches and consistent quantile scoring functions could improve results in cases where QCCD has limited power.

Second, the computational efficiency of QCCD is promising in the context of extensions to higher dimensional datasets. As such, ongoing research leverages existing graph discovery algorithms for hybrid learning as in Section 4. Furthermore, using QCCD and pair-copula constructions as building blocks for a novel approach to learn functional causal models is a promising area of further work.

References

Aue, A., Cheung, R. C. Y., Lee, T. C. M., and Zhong, M. (2014). Segmented Model Selection in Quantile Regression Using the Minimum Description Length Principle. *Journal of the American Statistical Association*, 109(109):507–1241.

Bauer, A. and Czado, C. (2016). Pair-copula Bayesian networks. *Journal of Computational and Graphical Statistics*, 25(4):1248–1271.

Budhathoki, K. and Vreeken, J. (2017). Causal inference by compression. In *ICDM*, pages 41–50.

Bühlmann, P., Peters, J., and Ernest, J. (2014). CAM: Causal additive models, high-dimensional order search and penalized regression. *Annals of Statistics*, 42(6):2526–2556.

Chang, Y., Li, Y., Ding, A., and Dy, J. (2016). A Robust-Equitable Copula Dependence Measure for Feature Selection. *AISTATS*, 41:84–92.

Chen, Z., Zhang, K., Chan, L., and Schölkopf, B. (2014). Causal discovery via reproducing kernel hilbert space embeddings. *Neural computation*, 26(7):1484–1517.

Cui, R., Groot, P., and Heskes, T. (2016). Copula PC algorithm for causal discovery from mixed data. In *Lecture Notes in Computer Science (including subseries Lecture Notes in Artificial Intelligence and Lecture Notes in Bioinformatics)*, volume 9852 LNAI, pages 337–392. Springer, Cham.

Elidan, G. (2013). Copulas in machine learning. In *Copulae in mathematical and quantitative finance*, pages 39–60. Springer.

Embrechts, P., Mcneil, E., and Straumann, D. (1999). Correlation: pitfalls and alternatives. *Risk Magazine*.

Fisher, R. A. (1936). Statistical methods for research workers. *Especially Section*, 21.

Geenens, G., Charpentier, A., and Paindaveine, D. (2017). Probit transformation for nonparametric kernel estimation of the copula density. *Bernoulli*, 23(3):1848–1873.

Gneiting, T. (2011). Making and Evaluating Point Forecasts. *Journal of the American Statistical Association*, 106(494):746–762.

Goudet, O., Kalainathan, D., Caillou, P., Lopez-Paz, D., Guyon, I., Sebag, M., Tritas, A., and Tubaro, P. (2017). Learning Functional Causal Models with Generative Neural Networks. *preprint*. <https://arxiv.org/pdf/1711.08936.pdf>.

Guennebaud, G., Jacob, B., and Others (2010). Eigen v3.

Hansen, M. H. and Yu, B. (2001). Model Selection and the Principle of Minimum Description Length. *Journal of the American Statistical Association*, 96(454):746–774.

Harrell Jr, F. E., with contributions from Charles Dupont, and others., M. (2017). Hmisc: Harrell Miscellaneous.

Harris, N. and Drton, M. (2013). PC Algorithm for Nonparanormal Graphical Models. *JMLR*, 14:3365–3383.

Heinze-Deml, C., Peters, J., and Meinshausen, N. (2017). Invariant Causal Prediction for Nonlinear Models. *preprint*. <https://arxiv.org/pdf/1706.08576.pdf>.

Hernández-Lobato, D., Morales Mombiela, P., Lopez-Paz, D., and Suárez, A. (2016). Non-linear causal inference using Gaussianity measures. *JMLR*, 17(1):939–977.

Hoyer, P. O., Janzing, D., Mooij, J., Peters, J., and Schölkopf, B. (2009). Nonlinear causal discovery with additive noise models. In *NIPS*, pages 689—696.

Janzing, D., Mooij, J., Zhang, K., Lemeire, J., Zscheischler, J., Daniusis, P., Steudel, B., and Schölkopf, B. (2012). Information-geometric approach to inferring causal directions. *Artificial Intelligence*, 182:1–31.

Janzing, D. and Schölkopf, B. (2010). Causal Inference Using the Algorithmic using Markov Condition. *IEEE Transactions on Information Theory*, 56(10):5168–5194.

Joe, H. (1996). Families of m-variate distributions with given margins and $m(m-1)/2$ bivariate dependence parameters. In *Distributions with fixed marginals and related topics*, pages 120–141. Institute of Mathematical Statistics.

Kolmogorov, A. N. (1963). On tables of random numbers. *Sankhyā: The Indian Journal of Statistics, Series A*, pages 369–376.

Liu, F. and Chan, L.-W. (2017). Causal Inference on Multidimensional Data Using Free Probability Theory. *IEEE transactions on neural networks and learning systems*.

Liu, H., Lafferty, J., and Wasserman, L. (2009). The Nonparanormal: Semiparametric Estimation of High Dimensional Undirected Graphs. *JMLR*, 10:2295–2328.

Lopez-Paz, D. (2016). *From Dependence to Causation*. PhD thesis, University of Cambridge.

Lopez-Paz, D., Hernandez-Lobato, J. M., and Schölkopf, B. (2013). Semi-Supervised Domain Adaptation with Copulas. *NIPS*, pages 674–682.

Lopez-Paz, D., Muandet, K., Schölkopf, B., and Tolstikhin, I. (2015). Towards a Learning Theory of Cause-Effect Inference. In *ICML*, pages 1452—1461.

Maathuis, M. H. and Nandy, P. (2016). A review of some recent advances in causal inference. In *Handbook of Big Data*. CRC Press.

Mandros, P., Boley, M., and Vreeken, J. (2017). Discovering reliable approximate functional dependencies. *KDD*, pages 355–364.

Marx, A. and Vreeken, J. (2017). Telling Cause from Effect using MDL-based Local and Global Regression. In *ICDM*.

Mooij, J. M., Peters, J., Janzing, D., Zscheischler, J., and Schölkopf, B. (2016). Distinguishing Cause from Effect Using Observational Data: Methods and Benchmarks. *JMLR*, 17:1–102.

Mooij, J. M., Stegle, O., Janzing, D., Zhang, K., and Schölkopf, B. (2010). Probabilistic latent variable models for distinguishing between cause and effect. In *NIPS*, pages 1687—1695.

Müller, D. and Czado, C. (2017). Selection of Sparse Vine Copulas in High Dimensions with the Lasso.

Nagler, T. and Vatter, T. (2017). vinecopulib: High Performance Algorithms for Vine Copula Modeling in C++. <http://vinecopulib.org>.

Nagler, T. and Vatter, T. (2018). *rvinecopulib*: High performance algorithms for vine copula modeling.

Pearl, J. (2009). *Causality*. Cambridge university press.

Pearl, J., Glymour, M., and Jewell, N. P. (2016). *Causal inference in statistics: A Primer*. John Wiley & Sons.

Peters, J. and Ernest, J. (2015). *CAM: Causal Additive Model (CAM)*.

Peters, J., Janzing, D., and Schölkopf, B. (2017). *Elements of causal inference : foundations and learning algorithms*. MIT Press (available on-line).

Peters, J., Mooij, J. M., Janzing, D., and Schölkopf, B. (2011). Identifiability of Causal Graphs using Functional Models. In *UAI*, pages 589—598.

Peters, J., Mooij, J. M., Janzing, D., and Schölkopf, B. (2014). Causal discovery with continuous additive noise models. *JMLR*, 15(1):2009–2053.

Pircalabelu, E., Claeskens, G., and Gijbels, I. (2017). Copula directed acyclic graphs. *Statistics and Computing*, 27(1):55–78.

R Core Team (2017). R: A Language and Environment for Statistical Computing.

Rasmussen, C. E. and Williams, C. K. I. (2006). *Gaussian processes for machine learning*, volume 1. MIT press Cambridge.

Rissanen, J. (1978). Modeling by shortest data description. *Automatica*, 14(5):465–471.

Scaillet, O., Charpentier, A., and Fermanian, J.-D. (2007). The estimation of copulas: Theory and practice. Technical report, Ensaes-Crest and Katholieke Universiteit Leuven, NP-Paribas and Crest; HEC Genve and Swiss Finance Institute.

Schäling, B. (2011). *The boost C++ libraries*.

Schölkopf, B., Janzing, D., Peters, J., Sgouritsa, E., Zhang, K., and Mooij, J. (2012). On Causal and Anticausal Learning. In *ICML*, pages 1255–1262.

Sgouritsa, E., Janzing, D., Hennig, P., and Schölkopf, B. (2015). Inference of Cause and Effect with Unsupervised Inverse Regression. In *AISTATS*, pages 847—855.

Shimizu, S., Patrik Hoyer, I. O., and Antti, K. (2006). A Linear Non-Gaussian Acyclic Model for Causal Discovery Aapo Hyvärinen. *JMLR*, 7:2003–2030.

Sklar, A. (1959). Fonctions de répartition à n dimensions et leurs marges. *Publications de L'Institut de Statistique de L'Université de Paris*, 8:229–231.

Smyth, G. K. (2005). Numerical integration. *Encyclopedia of Biostatistics*, pages 3088–3095.

Spirites, P. and Zhang, K. (2016). Causal discovery and inference: concepts and recent methodological advances. *Applied Informatics*, pages 165—191.

Tran, D., Blei, D. M., and Airoldi, E. M. (2015). Copula variational inference. In *NIPS*, pages 3564–3572.

Turing, A. M. (1937). On computable numbers, with an application to the Entscheidungsproblem. *Proceedings of the London mathematical society*, 2(1):230–265.

Turing, A. M. (1938). On computable numbers, with an application to the Entscheidungsproblem. A correction. *Proceedings of the London Mathematical Society*, 2(1):544–546.

Zhang, K. and Hyvärinen, A. (2009). On the Identifiability of the Post-Nonlinear Causal Model. In *UAI*, pages 647—655.

6 Supplementary Material

6.1 Example simulated datasets

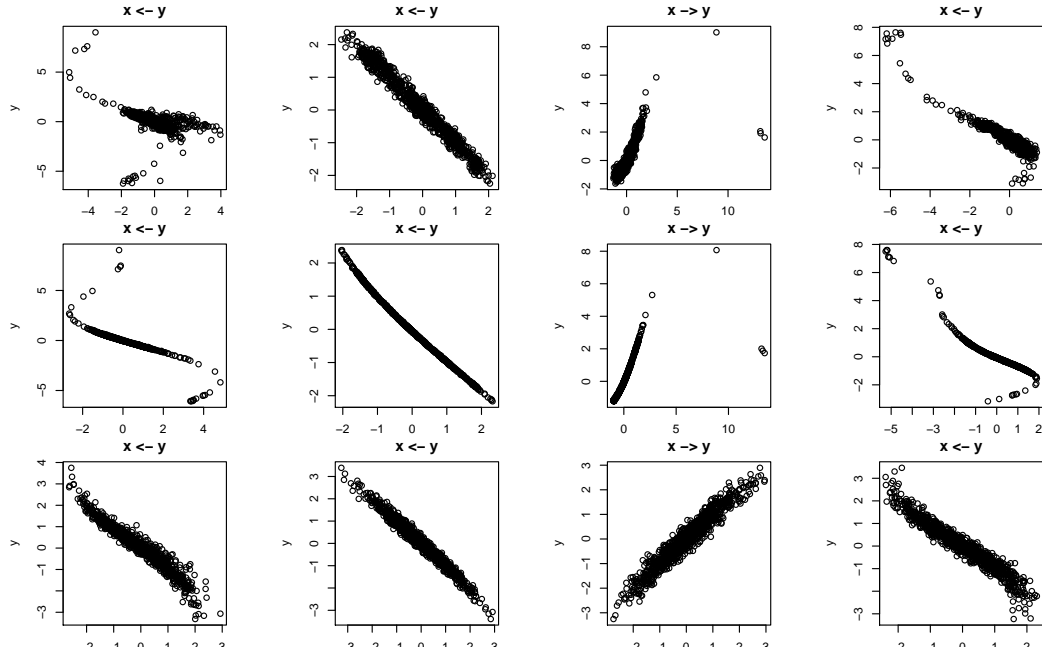


Figure 6: SIM/SIM- \ln /SIM-G (first/second/third row).

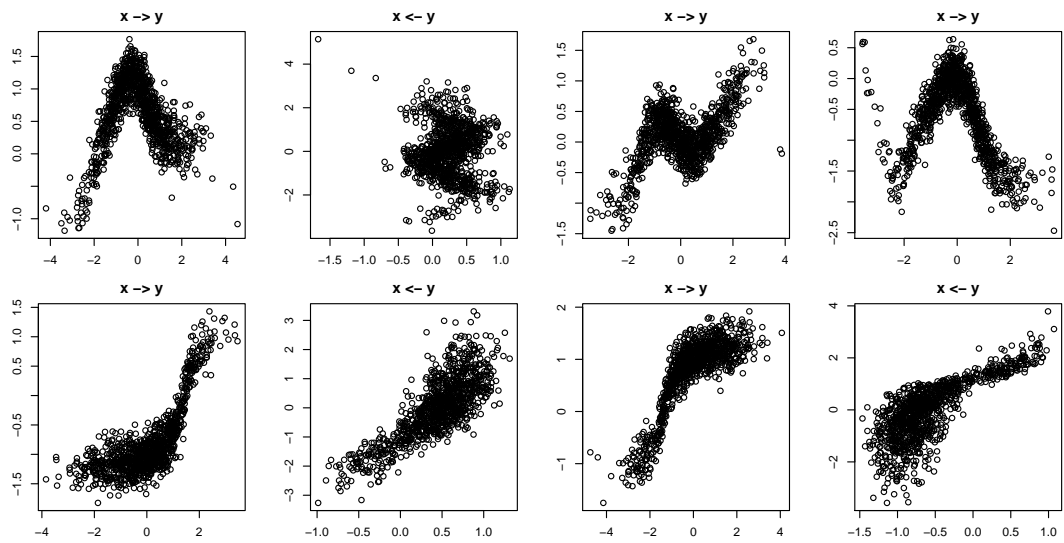


Figure 7: AN/AN-s (first/second row).

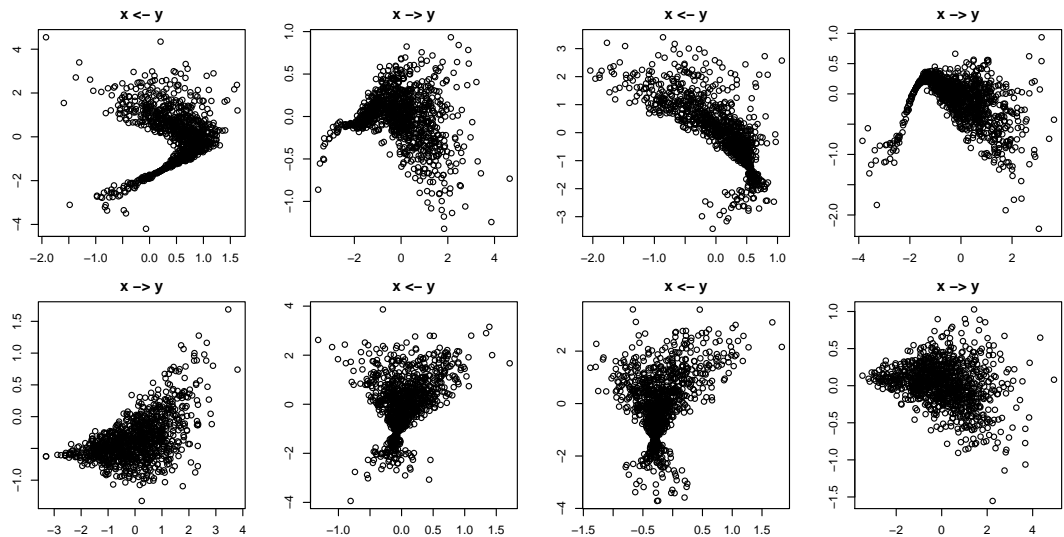


Figure 8: HN/HN-s (first/second row).

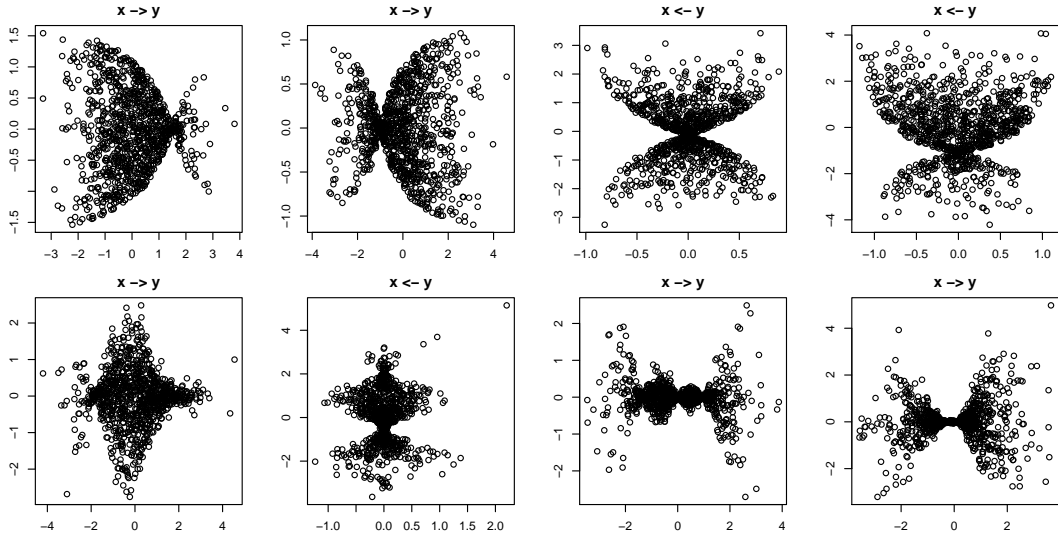


Figure 9: MN-U/MN-G (first/second row).

6.2 Additional results from experiments

Table 5: Area under ROC curve on simulated data.

	SIM	SIM-Ln	SIM-G	AN	AN-s	HS	HS-s	MN-U	MN-G
QCCD	0.55	0.89	0.89	1	1	1	1	1	0.91
IGCI	0.38	0.56	0.56	0.39	0.39	0.9	0.94	0	0.99
biCAM	0.62	0.85	0.89	1	1	0.78	0.47	0	0.57
Slope	0.47	0.44	0.45	0.09	0.23	0.65	0.83	0	0.99
RESIT	0.78	0.85	0.75	1	1	0.4	0	0.52	0.52
LINGAM	0.53	0.54	0.5	0.48	0.56	0.62	0.46	0.49	0.52
EMD	0.44	0.44	0.61	0.37	0.5	0.81	0.91	0.72	0.99
GR-AN	0.56	0.5	0.66	0.03	0.01	0.12	0.5	0.97	0.38

Table 6: Area under PR curve on simulated data.

PR	SIM	SIM-Ln	SIM-G	AN	AN-s	HN	HN-s	MN-U	MN-G
QCCD	0.6	0.89	0.89	1	1	1	1	1	0.93
IGCI	0.42	0.52	0.63	0.55	0.44	0.9	0.94	0.3	0.99
biCAM	0.63	0.84	0.83	1	1	0.8	0.48	0.33	0.59
Slope	0.5	0.48	0.5	0.36	0.37	0.69	0.83	0.29	0.99
RESIT	0.72	0.78	0.72	1	1	0.49	0.31	0.50	0.44
LINGAM	0.54	0.54	0.5	0.56	0.47	0.59	0.5	0.46	0.58
EMD	0.45	0.45	0.61	0.52	0.58	0.81	0.91	0.72	0.99
GR-AN	0.61	0.56	0.66	0.35	0.32	0.32	0.5	0.97	0.46

6.3 Octet dataset pairwise results

Table 7: Number of correct decision for the Octet dataset.

	QCCD	ICGI	biCAM	Slope	RESIT	LINGAM	EMD	GRAN
#correct dec.	10/10	9/10	4/10	9/10	4/10	3/10	10/10	9/10

6.4 Computational complexity

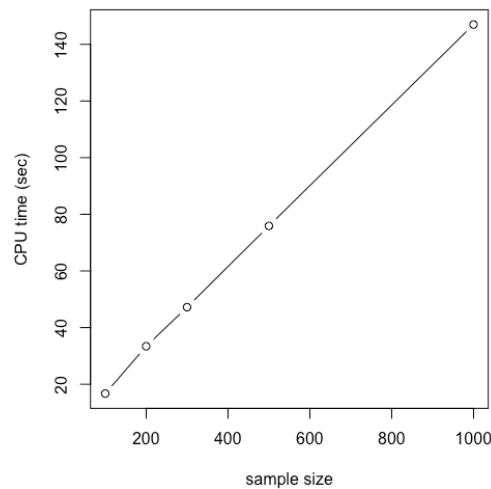


Figure 10: Linear scaling of QCCD over 100 pairs, $m = 1$, n varies.